

# Efficient generation of graph states for quantum computation

S. R. Clark,<sup>1</sup> C. Moura Alves,<sup>1,2</sup> and D. Jaksch<sup>1</sup>

<sup>1</sup>Clarendon Laboratory, University of Oxford, Parks Road, Oxford OX1 3PU, U.K.

<sup>2</sup>DAMTP, University of Cambridge, Wilberforce Road, Cambridge CB3 0WA, U.K.

(Dated: November 7, 2018)

We present an entanglement generation scheme which allows arbitrary graph states to be efficiently created in a linear quantum register via an auxiliary entangling bus. The dynamics of the entangling bus is described by an effective non-interacting fermionic system undergoing mirror-inversion in which qubits, encoded as local fermionic modes, become entangled purely by Fermi statistics. We discuss a possible implementation using two species of neutral atoms stored in an optical lattice and find that the scheme is realistic in its requirements even in the presence of noise.

PACS numbers: 03.67.Mn, 03.67.Lx

Bipartite entanglement has long been recognized as a useful physical resource for tasks such as quantum cryptography and quantum teleportation. Similarly, multipartite entanglement is an essential ingredient for more complex quantum information processing (QIP) tasks, and interest in this resource has grown since its controlled generation was demonstrated in several physical systems [1, 2]. An important class of multipartite entangled states are graph states. By using vertices in a graph to represent qubits, and edges to represent an Ising type interaction that has taken place between two qubits, the graph formalism gives an effective characterization of entanglement by the presence of edges [3]. Special instances of graph states are the resource used in multi-party communication protocols, in quantum error correcting codes [4] and in one-way quantum computing [5].

Initial proposals for the generation of graph states in physical systems focussed on qubit lattices of fixed geometry, where each qubit interacts only with its nearest-neighbors [3]. Such a scheme has been experimentally implemented in 1D with optical lattices of neutral atoms via controlled collisions [1]. The graph states generated with this method follow the geometry of the lattice, and for 2D/3D square lattices they constitute, together with single qubit measurements, a universal resource for quantum computation [5]. However, the generation of more complex graphs, where the set of edges does not translate into a regular arrangement of qubits, e.g. the quantum Fourier transform graph state, requires the ability to pre-engineer a complicated geometry of the qubit interactions. A simple scheme in which any graph state can be created in a set of qubits with a regular fixed geometry is therefore highly desirable, and some progress has been made towards this with non-deterministic linear optical protocols [6].

In this paper we propose a scheme for efficiently generating arbitrary graph states within a linear quantum register via an auxiliary entangling bus (EB). The EB is a fixed ‘always on’ system, equivalent, in a specific limit, to a non-interacting fermionic system where qubits trans-

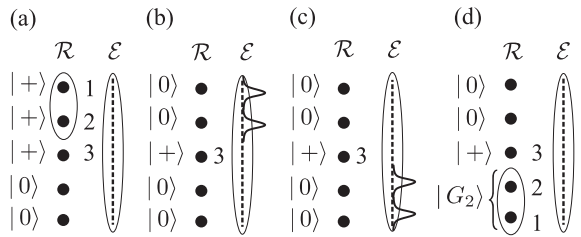


FIG. 1: (a) Consider a quantum register  $\mathcal{R}$  which has 3 graph qubits in a state  $|+\rangle$ . (b) Two of them are transferred to the EB  $\mathcal{E}$  where their state is mapped into local fermionic modes. (c)  $\mathcal{E}$  evolves via  $H_f$  for time  $\tau$ , which results in the mirror-inversion of the two qubits. (d) The qubits at the mirror-inverted location are transferred back to  $\mathcal{R}$ , yielding a graph state with 2 vertices  $|G_2\rangle$ . Repeating this procedure with different qubits allows any 3-qubit graph state to be generated in  $\mathcal{R}$ .

ferred from the register subsequently become encoded as local fermionic modes (LFMs) [7]. The dynamics of the EB over a fixed time then result in the complete mirror-inversion of these LFMs yielding robust phases within its fermionic state purely as a consequence of Fermi statistics. Upon transferring the mirror-inverted LFMs back to the register the EB has generated entanglement between the qubits. For two qubits this procedure performs a controlled- $\sigma_z$  ( $c\sigma_z$ ) gate, in addition to the inversion [8], as depicted in Fig. 1, and this is sufficient to establish an edge between the vertices that these qubits represent [3]. We examine an implementation of this scheme where the EB is an XY spin chain formed from an optical lattice of neutral atoms and investigate numerically its fidelity in the presence of noise. Finally we describe how, through the effective quantum circuit implemented by transferring and evolving more than two qubits within the EB for the same fixed time, arbitrary graph states of  $n$  vertices can be generated in at most  $O(2n)$  EB cycles. This represents an improvement over the  $O(n^2)$  steps required in a network model composed of two-qubit gates.

The starting point for our implementation of the EB is a 1D optical lattice of ultracold bosonic atoms in two

long-lived internal (hyperfine) states  $|a\rangle$  and  $|b\rangle$ . The dynamics of this system over  $N$  sites is then described by a two-species Bose-Hubbard model (BHM) given by [9]

$$H = \sum_{n=1}^N \left( \frac{U_n^a}{2} a_n^\dagger a_n^2 + \frac{U_n^b}{2} b_n^\dagger b_n^2 + U_n^{ab} a_n^\dagger a_n b_n^\dagger b_n \right) - \sum_{n=1}^{N-1} (t_n^a a_n^\dagger a_{n+1} + t_n^b b_n^\dagger b_{n+1} + \text{H.c.}) + H_B, \quad (1)$$

where  $a_n(b_n)$  is the bosonic destruction operator for an  $a(b)$ -atom in the  $n$ th site, and  $H_B = (B/2) \sum_n (a_n^\dagger a_n - b_n^\dagger b_n)$  is the contribution of a uniform external field. The parameters  $t^{a(b)}$  and  $U^{a(b)}$ ,  $U^{ab}$  are the laser-intensity-dependent hopping matrix elements and on-site interactions for atoms in states  $|a\rangle$  ( $|b\rangle$ ) respectively. These parameters will in general have a spatial profile across the lattice. The dynamic controllability and long decoherence times of this system have made it of considerable interest for QIP [10, 11] and for realizing spin models [9].

We focus on the two-species BHM in the limit of large interactions,  $U^a, U^b, U^{ab} \gg t^a, t^b$ , which energetically prohibit the multiple occupancy of any site. Hopping can be then treated perturbatively and to lowest order, for an initial Mott insulating state with commensurate filling of one atom per lattice site, the effective Hamiltonian is found to be [9]

$$H_s = \sum_{n=1}^{N-1} \lambda_n^{zz} \sigma_n^z \sigma_{n+1}^z + \lambda_n^z \sigma_n^z - \lambda_n^{xy} (\sigma_n^x \sigma_{n+1}^x + \sigma_n^y \sigma_{n+1}^y). \quad (2)$$

Hence we obtain the anisotropic Heisenberg spin model in the optical lattice, with  $|a\rangle \equiv |\uparrow\rangle$  and  $|b\rangle \equiv |\downarrow\rangle$  at each site. The corresponding Pauli operators are then  $\sigma_n^z = a_n^\dagger a_n - b_n^\dagger b_n$ ,  $\sigma_n^x = a_n^\dagger b_n + b_n^\dagger a_n$ ,  $\sigma_n^y = -i(a_n^\dagger b_n - b_n^\dagger a_n)$ , while the couplings are given by  $\lambda_n^{zz} = (t_n^{a2} + t_n^{b2})/(2U_n^{ab}) - t_n^{a2}/U_n^a - t_n^{b2}/U_n^b$ ,  $\lambda_n^z = 4(t_n^{a2}/U_n^a - t_n^{b2}/U_n^b) + B/2$ , and  $\lambda_n^{xy} = t_n^a t_n^b / U_n^{ab}$ . The construction of the EB requires the optical lattice parameters to be engineered such that  $U_n^a = U_n^b = 2U_n^{ab}$  and  $t_n^a = t_n^b$ , thereby ensuring that  $\lambda_n^{zz} = 0$ ,  $\lambda_n^z = B/2$ , and that  $H_s$  reduces to a pure XY spin chain. For simplicity we assume that only the hopping possesses spatial dependence via  $t_n^a = t_n^b = T\sqrt{\alpha_n}$ , with a profile obeying  $0 < \alpha_n \leq 1$  so  $\max(t_n^{a(b)}) \leq T$ , and that the interaction energies are constant over the system as  $U^a = U^b = 2U^{ab} = U$  with both  $U$  and  $T$  constants. To first order in  $T/U$  the dynamics of the optical lattice reduces to an XY spin chain with couplings  $\lambda_n^{xy} = (2T^2/U)\alpha_n$ . For the moment we shall assume ideality where  $U/T \gg 1$ ; however, later we will investigate how the fidelity of this mapping varies with  $U/T$  and in the presence of noise.

It is well known that the Jordan Wigner transformation (JWT) [12] maps the XY spin chain to a non-interacting fermionic Hamiltonian  $H_f = -\sum_n j_n (c_n^\dagger c_{n+1} + c_{n+1}^\dagger c_n) + \sum_n u_n c_n^\dagger c_n$ , where  $j_n =$

$2\lambda_n^{xy}$ ,  $u_n = B$ , and  $c_n$  is a fermionic destruction operator for the  $n$ th site obeying the usual anticommutation relations. We are particularly interested in the *angular momentum* hopping profile [13] given by  $j_n = (J/2)\sqrt{n(N-n)}$ , which we write as  $j_n = W\alpha_n$  with  $\alpha_n = 2\sqrt{(n/N)[1-(n/N)]}$  and  $W = 4T^2/U = JN/4$  so  $\max(j_n) \leq W$ . In this case the projection of  $H_f$  onto the single fermion subspace of the lattice,  $\mathcal{H}_1$ , results in a Hamiltonian equivalent to  $H_1 = -JS_x + B\mathbb{1}$ , where  $S_x$  is the  $x$  angular momentum operator for an ‘effective’ spin- $\mathcal{S}$  particle, with  $\mathcal{S} = (N-1)/2$ . The single-fermion states  $\{|n\rangle = c_n^\dagger |\text{vac}\rangle\}$  then correspond to the  $z$ -angular momentum eigenstates  $\{|\mathcal{S}, l\rangle_z\}$  of the spin- $\mathcal{S}$  particle, with  $|1\rangle = |\mathcal{S}, -\mathcal{S}\rangle_z, \dots, |N\rangle = |\mathcal{S}, \mathcal{S}\rangle_z$ . The dynamics generated in  $\mathcal{H}_1$ , when  $H_1$  is applied for a fixed time  $\tau = \pi/J$ , result in the time-evolution unitary  $U_1(\tau) = \exp(i\phi_B) \exp(i\pi S_x)$  composed of an overall phase  $\phi_B = -B\pi/J$  for  $\mathcal{H}_1$  and a rotation of the spin- $\mathcal{S}$  particle about the  $x$ -axis by  $\pi$ . This leads directly to perfect state transfer over the lattice [13]. The action of  $U_1(\tau)$  on the single-particle basis follows from its equivalence to the  $z$ -angular momentum states where  $\exp(i\pi S_x) |\mathcal{S}, l\rangle_z = \exp(i\pi \mathcal{S}) |\mathcal{S}, -l\rangle_z$ . Thus we find that  $U_1(\tau) |n\rangle = \exp(i\phi_1) |\bar{n}\rangle$ , with the phase  $\phi_1 = \pi\mathcal{S} + \phi_B$  and mirror-conjugate location  $\bar{n} = N - n + 1$ . Choosing  $B = \mathcal{S}J$  is sufficient to ensure that the single-particle phase  $\phi_1$  vanishes. The evolution of the fermionic modes  $c_n^\dagger$  then satisfies  $U c_n^\dagger U^\dagger = c_{\bar{n}}^\dagger$ , where  $U = \exp(-iH_f\tau)$ , and the dynamics of the system describe the complete mirror-inversion of the LFM.

Under the JWT the  $N$  qubit (or spin) states  $|q_1, \dots, q_N\rangle$ , with  $q_n \in \{0, 1\}$ , of the chain are mapped to Fock states of the LFM as  $|q_1, \dots, q_N\rangle = (c_1^\dagger)^{q_1} \dots (c_N^\dagger)^{q_N} |\text{vac}\rangle$  (using lattice operator ordering) which describe the occupancy of the system by quasi-fermions. The use of fermionic mode occupancy as a basis for quantum computation has been proposed before [7]. Complications arise since the accessibility of the Fock space of real fermions is restricted by *superselection* rules, and also, in contrast to bosons, it does not possess a natural tensor product structure permitting independent operations on each mode, thus making it intrinsically nonlocal [14]. However, since we have focussed on a physical system which *maps* to a non-interacting fermionic system, the Fock space is fully accessible, thus enabling superpositions of states with different numbers of quasi-fermions, which are essential for encoding qubits.

For systems of identical fermions a bilinear fermionic Hamiltonian such as  $H_f$  suffices to generate mode entanglement, despite describing a non-interacting system [15]. The entanglement generated by mirror-inversion then follows straightforwardly from Fermi statistics through its action on Fock states as

$$e^{-iH_f\tau} |q_1, \dots, q_N\rangle = e^{-i\pi\Sigma_Q} |q_N, \dots, q_1\rangle, \quad (3)$$

where  $\Sigma_Q$  is the number of anti-commutations of the op-

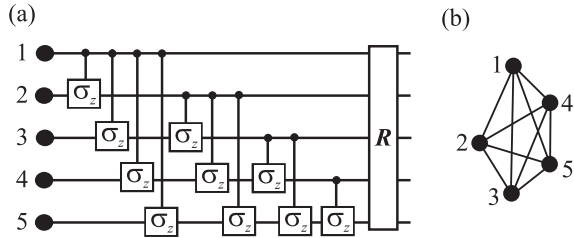


FIG. 2: For 5 qubits we have (a) the quantum circuit  $\mathcal{C}(5)$  equivalent to the dynamics of  $H_f$  for a time  $\tau$ , and (b) the fully connected graph state  $|G_5\rangle$  with 5 vertices generated by this circuit if all the qubits are initialized in the  $|+\rangle$  state. Both the circuit and the resulting graph state generalize in an obvious way for more qubits.

erators  $c_n^\dagger$  required to reestablish a Fock state. Specifically  $\Sigma_Q = Q(Q - 1)/2$ , where  $Q$  is the number of fermions, i.e.  $Q = \sum_{n=1}^N c_n^\dagger c_n = \sum_{n=1}^N q_n$ , and so phases are only acquired between subspaces with different  $Q$ . Since Eq. (3) is written in terms of Fock states, the inverse-JWT removes the antisymmetry when mapping back to qubits, while leaving the phases acquired between fermion-number (or total magnetization) subspaces untouched. Thus the evolution of the EB over a fixed time  $\tau$  is equivalent to a quantum circuit  $\mathcal{C}(N)$  composed of  $c\text{-}\sigma_z$  gates between all distinct pairs of  $N$  qubits followed by the inversion operator  $R$ , as shown in Fig. 2(a) for  $N = 5$ . Usefully, if  $N - q$  qubits are in the state  $|0\rangle$ , then this circuit reduces to  $\mathcal{C}(q)$  between the remaining  $q$  qubits, independent of their locations, followed by the full inversion  $R$ .

In passing we note that the above results apply to more general settings. Suppose we partition the fermionic lattice into  $M$  equal blocks, each labelled by their central site  $k$ , and composed of sites  $m(k)$ . Within each block  $k$  we consider an extended fermionic mode  $f_k^\dagger = \sum_{n \in m(k)} \phi_n^k c_n^\dagger$ , defined by a single-particle state  $\phi_n^k$  contained entirely within the block  $k$  and symmetrical about its center. The dynamics of the EB over some fixed time will be equivalent to  $\mathcal{C}(M) R$  as long as  $j_n$  and  $u_n$  are chosen such that the dynamics of  $H_f$  performs mirror-inversion with respect to  $f_k^\dagger$ . We can equally consider partitioning a 1D continuous fermionic system, described by field operators  $\hat{\psi}^\dagger(x)$ , and defining extended LFMAs analogously as  $f_k^\dagger = \int_{m(k)} dx \phi^k(x) \hat{\psi}^\dagger(x)$ , with  $\phi^k(x) = 0, \forall x \notin m(k)$ . In this case, harmonic trapping  $V(x) = m\omega^2 x^2/2$  and Gaussian modes  $f_k^\dagger$  are sufficient for mirror-inversion over a time  $\tau = \pi/\omega$ , giving an arrangement conceptually similar to the 1D cold-collision proposal in [16] at the Tonks-Girardeau limit [17].

The generation of arbitrary graph states requires the EB to be augmented with a linear register of  $N$  qubits, and a transfer process which maps a qubit state into a LFM in the EB via  $\sigma_n^+ \mapsto c_n^\dagger$ , where  $\sigma_n^+$  is the Pauli ladder operator. The register and the EB are then ini-

tialized in the states  $\otimes_i^N |0\rangle_i$  and  $|\text{vac}\rangle$  respectively. The scheme begins by choosing a set of register qubits  $\Gamma$  to be the graph vertices, and applying a Hadamard transformation to each of them:  $|0\rangle \rightarrow |+\rangle = (|0\rangle + |1\rangle)/\sqrt{2}$ , as in Fig. 1(a) for qubits 1 – 3. A subset  $\Sigma$  of  $m$  of these qubits is then transferred to the EB and allowed to evolve for a time  $\tau$ , as shown (for  $m = 2$ ) in Fig. 1(b) and Fig. 1(c) for qubits 1 and 2. The LFM qubits within the EB at the corresponding mirror-inverted locations  $\bar{\Sigma}$  are then transferred back to the register, yielding a fully connected graph state  $|G_m\rangle$  between these  $m$  vertices, as in Fig. 1(d). Such a state is locally equivalent to a  $m$ -qubit GHZ state, as depicted in Fig. 2(b) for  $m = 5$ . Overlap between EB and register graph qubits can be avoided by choosing  $|\Gamma| = [N/2]$  with locations in the first half of the register.

Our system can generate any graph state of  $n$  vertices in at most  $O(n^2)$  steps by utilizing only the two-qubit interaction of the EB to establish each edge individually, mimicking the network model of two-qubit gates. However, by exploiting the multi-qubit circuit implemented by the EB dynamics over the same time  $\tau$ , as in Fig. 2(a), our scheme can improve this upper bound. Specifically, we proceed iteratively with  $g = 1$  by (i) transferring the  $g$ th graph qubit, and all graph qubits  $g_c > g$  which will connect to  $g$ , into the EB; (ii) allowing them to evolve for a time  $\tau$  creating a complete set of connections between these vertices, c.f. Fig. 2(b); (iii) then transferring qubit  $g$  back to the register while leaving the qubits  $g_c$  to evolve for one cycle longer in the EB, subsequently removing all the connections between them; (iv) and finally transferring the qubits  $g_c$  back to the register and repeating step (i) with  $g \mapsto g + 1$ . Thus, any graph of  $g = n$  vertices can be generated in at most  $O(2n)$  uses of the EB.

In the optical lattice implementation, both the register and the EB are effective spin chains. The register is created by turning off the hopping completely [11] and is separated from the EB by a potential barrier (see [18] for details of this setup). The transfer process between the register and EB can then be accomplished either directly via state-independent tunnelling [18, 19], or through the implementation of a swap gate between the register and EB qubits [10], on a time scale much faster than  $\tau$ .

We considered some dominant sources of imperfections within the optical lattice EB. In particular, we investigated the fidelity of the two-species BHM to spin-chain mapping introduced earlier, for finite  $U/T$ . We considered a system of size  $N = 6$  initialized in a product state  $|+\rangle \otimes |0\rangle^{\otimes 4} \otimes |+\rangle$ , and computed the exact time-evolution of the two-species BHM using the time-evolving block decimation (TEBD) algorithm [20] for varying  $U/T$  over the appropriate inversion time  $\tau$ . Using the effective two-spin density matrix for the end sites, the fidelity  $F$  was computed with the state  $|G_2\rangle$  obtained from a perfectly implemented XY chain. The simulation results in Fig. 3(a) demonstrate that, as expected, the fidelity in-

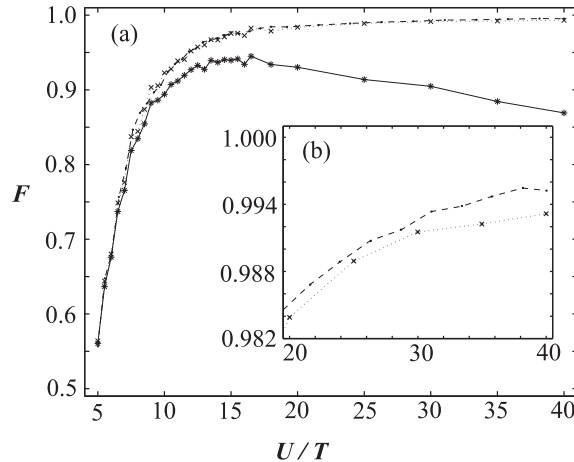


FIG. 3: (a) The fidelity  $F$  of the effective XY spin-chain implemented by the 2-species BHM with the ratio  $U/T$ , for no noise  $\Delta = 0$  (·),  $\Delta = 1\%$  (×) and  $\Delta = 5\%$  (\*). (b) A close-up of (a). The solid, dashed and dotted lines are drawn to guide the eye.

creases with  $U/T$ . Given that  $\tau = UN\pi/16T^2$ , increasing the fidelity, by deepening the lattice, comes at the cost of longer inversion times. However, Fig. 3(b) shows that  $F > 0.99$  even at a moderate ratio of  $U/T = 26$ . At this depth a  $\lambda = 514$  nm optical lattice of  $^{23}\text{Na}$  atoms has  $\tau = 9.3$  ms, while a  $\lambda = 826$  nm optical lattice of  $^{87}\text{Rb}$  atoms has  $\tau = 79$  ms. These are fast enough for multiple EB inversions to occur within the decoherence time of the system, which is typically of order of a second [19].

Finally, we investigated the effect of jitter in the lattice laser intensities. For  $^{87}\text{Rb}$  the laser intensities  $I_a$  and  $I_b$  of the  $a$  and  $b$  lattices were taken as varying independently according to some Wiener noise  $dW_{a(b)}(t)$  with variance  $\Delta^2$ :  $I_{a(b)}(t) = I_0 + dW_{a(b)}(t)$ , where  $I_0$  is the ideal laser intensity. Such laser fluctuations are then non-linearly related to the corresponding fluctuations in the hopping  $t_n^{a(b)}$  and on-site interaction  $U^{a(b)}$ ,  $U^{ab}$  matrix elements of the 2-species BHM [19]. We assumed a simplified version of this noise in which the fluctuations alter the hopping and interaction scalings  $T$  and  $U$  contained within the overall scaling  $W$  of  $j_n$ , but not the spatial profile  $\alpha_n$ . Despite this restriction, this noise causes fluctuations in the inversion time  $\tau$  during the dynamics, and also breaks the symmetry required to ensure that no  $\sigma_n^z \sigma_{n+1}^z$  or spatially-varying  $\sigma_n^z$  contributions occur. In Fig. 3(a) the fidelity curves are plotted for  $\Delta = 1\%$  and  $\Delta = 5\%$  of  $I_0$ . For  $\Delta = 5\%$  the fidelity is seen to drop off in deeper lattices due to the cumulative effect of noise over longer inversion times. Crucially, the fidelity curve suffers only a minimal reduction due to  $\Delta = 1\%$  noise, as in Fig. 3(b), and this represents a realistic value for the experimental stabilization of the laser intensity.

We have shown how arbitrary Graph states can be gen-

erated efficiently by using an EB whose dynamics correspond to a non-interacting fermionic system undergoing mirror-inversion. By utilizing an EB which is fixed and always on the dynamical control required for QIP tasks can be reduced to single qubit operations. Here an implementation of this scheme using an optical lattice of neutral atoms was considered in detail. We also note that the EB properties are well suited to solid state systems. The fidelity of the optical lattice proposal was examined not only for the depth ratio  $U/T$ , but also in the presence of noise, and found to be both realistic and robust.

This work was supported by the EPSRC IRC network on Quantum Information Processing (U.K.). S.C. and D.J. thank Peter Zoller and Hans Briegel for stimulating discussions. C.M.A. thanks Marc Hein for insightful discussions on graph states and is supported by the Fundação para a Ciência e Tecnologia (Portugal).

---

- [1] O. Mandel *et al.*, *Nature (London)* **425**, 937 (2003).
- [2] P. Walther *et al.*, *Nature (London)* **429**, 158 (2004); C.A. Sackett *et al.*, *ibid* **404**, 256 (2000); A. Rauschenbeutel *et al.*, *Science* **288**, 2024 (2000).
- [3] M. Hein, J. Eisert and H.-J. Briegel, *Phys. Rev. A* **69**, 062311 (2004).
- [4] D. Gottesman, Ph.D thesis (CalTech, Pasadena, 1997); A.M. Steane *Phys. Rev. Lett.* **77**, 793 (1996).
- [5] R. Raussendorf and H.-J. Briegel, *Phys. Rev. Lett.* **86**, 910 (2001); R. Raussendorf and H.-J. Briegel, *Phys. Rev. Lett.* **86**, 5188 (2001).
- [6] D.E. Browne and T. Rudolph, e-print quant-ph/0405157; S.D. Barrett and P. Kok, e-print quant-ph/0408040.
- [7] S.B. Bravyi and A.Y. Kitaev, *Ann. Phys. (San Diego)* **298**, 210 (2002).
- [8] M.-H. Yung and S. Bose, *Quan. Inf. & Comp.* **4**, 174 (2004); M.-H. Yung and S. Bose, e-print quant-ph/0407212.
- [9] L.-M. Duan, E. Demler and M.D. Lukin, *Phys. Rev. Lett.* **91**, 090402 (2003); J.J. García-Ripoll and J.I. Cirac, *New J. Phys.* **5**, 76.1 (2003).
- [10] J.K. Pachos and P.L. Knight, *Phys. Rev. Lett.* **91**, 107902 (2003).
- [11] D. Jaksch and P. Zoller, e-print cond-mat/0410614.
- [12] See for example, S. Sachdev, *Quantum Phase Transitions* (Cambridge Univ. Press, Cambridge, 2001).
- [13] M. Christandl *et al.*, *Phys. Rev. Lett.* **92**, 187902 (2004).
- [14] P. Zanardi, *Phys. Rev. A* **65**, 042101 (2002); L.-A. Wu and D.A. Lidar, *J. Math. Phys.* **43**, 4506 (2002).
- [15] V. Vedral, *Central Eur. J. Phys.* **1**, 289 (2003).
- [16] T. Calarco *et al.*, *Fortschritte der Physik* **48**, 945 (2000).
- [17] B. Paredes *et al.*, *Nature (London)* **429**, 277 (2004).
- [18] C. Moura Alves and D. Jaksch, *Phys. Rev. Lett.* **93**, 110501 (2004).
- [19] M. Greiner *et al.*, *Nature (London)* **415**, 39 (2002); W.K. Hensinger *et al.*, *ibid* **412**, 52 (2001); D. Jaksch *et al.* *Phys. Rev. Lett.* **81**, 3108 (1998).
- [20] G. Vidal, *Phys. Rev. Lett.* **91**, 147902 (2003).